Toolbox

Editor's Note: Toolboxes are intended to briefly highlight a new method or a resource of general use in neuroscience or to critically analyze existing approaches or methods. For more information, see http://www.jneurosci.org/misc/itoa.shtml.

Surface Trafficking of Neurotransmitter Receptor: Comparison between Single-Molecule/Quantum Dot Strategies

Laurent Groc,[1] Mathieu Lafourcade,[1] Martin Heine,[1] Marianne Renner,[1] Victor Racine,[3] Jean-Baptiste Sibarita,[3] Brahim Lounis,[2] Daniel Choquet,[1] and Laurent Cognet[2]

[1]Physiologie Cellulaire de la Synapse, Unité Mixte de Recherche (UMR) 5091, Centre National de la Recherche Scientifique (CNRS), Université Bordeaux 2, 33077 Bordeaux, France, [2]Centre de Physique Moléculaire Optique et Hertzienne, UMR 5798, CNRS, Université Bordeaux 1, 33405 Talence, France, and [3]Curie Institute, Research Division, UMR 144-CNRS, 75005 Paris, France

The cellular traffic of neurotransmitter receptors has captured a lot of attention over the last decade, mostly because synaptic receptor number is adjusted during synaptic development and plasticity. Although each neurotransmitter receptor family has its own trafficking characteristics, two main modes of receptor delivery to the synapse have emerged: endo-exocytotic cycling and surface diffusion [e.g., for glutamatergic receptors, see Bredt and Nicoll (2003) and Groc and Choquet (2006)]. Receptor cycling through endo-exocytotic processes can be measured by several experimental means, from biochemical to imaging assays. The use of fluorescent protein (XFP)-tag imaging provides a powerful approach to investigate the trafficking of receptor clusters between neuronal compartments (e.g., soma, dendrite, spine) (Kennedy and Ehlers, 2006). A disadvantage of the XFP-tag approach in live experiment is extreme difficulty in detecting XFP fluorescence signals from small nonclustered receptor pool (Cognet et al., 2002; Lippincott-Schwartz and Patterson, 2003). XFP-tagged neurotransmitter receptors are often present in several cellular compartments from the endoplasmic reticulum to the plasma membrane with various relative contents. For instance, surface XFP-tagged neurotransmitter receptors represent only a minor fraction of the total receptor population, precluding their specific detection. Alternative live-cell imaging approaches were thus required to specifically isolate surface receptors. Interestingly, a variant of the green fluorescent protein (GFP), ecliptic pHluorin, shows a reversible excitation ratio change between pH 7.5 and 5.5, and its absorbance decreases as the pH is lowered. Most neurotransmitter receptors, including the ionotropic glutamate ones, display an extracellular N-terminal region, implying that the N terminus will always be in an acidic environment inside the cell, whereas it will be exposed to a neutral pH after insertion into the plasma membrane. By this means, surface receptors can be specifically detected and tracked with live-imaging approaches (Ashby et al., 2004). Alternatively, surface receptors can be labeled and detected by immunocytochemical approaches using antibodies directed against receptor extracellular epitopes.

The purpose of this Toolbox is to outline currently available approaches to measure the surface trafficking of receptor in neurons, with a special emphasis on single-molecule (organic dye) and quantum dot (QDot) detection for neurotransmitter receptor tracking.

Exploring receptor surface trafficking: approaches

Investigation of receptor surface distribution and diffusion can be sorted in two groups. On the one hand, the average surface diffusion of labeled receptors is studied without distinction of individual behaviors (Fig. 1*A*). Surface receptors can be isolated by electrophysiologically tagged methods (Tovar and Westbrook, 2002; Adesnik et al., 2005; Thomas et al., 2005). Schematically, a subpopulation of surface receptors is irreversibly blocked (e.g., MK-801 for NMDA receptors) and the receptor surface diffusion is estimated from time-dependent functional recovery after receptor blockade. Another approach is based on the fluorescence labeling techniques coupled to live fluorescence microscopy, such as fluorescent recovery after photobleaching (FRAP) of pHluorin-tagged receptors (Rasse et al., 2005; Ashby et al., 2006; Kopec et al., 2006; Lober et al., 2006; Sharma et al., 2006). Note that both

Received April 11, 2007; revised Sept. 18, 2007; accepted Oct. 2, 2007.

This work was supported by grants from the Centre National de la Recherche Scientifique, Conseil Régional d'Aquitaine, Ministère de la Recherche, and Fondation pour la Recherche Médicale and by a European Community Grant (GRIPANT, CT-2005-005320). We thank Richard Huganir for the cDNA BGG construct and Christelle Breillat, Beatrice Teissier, and Delphine Bouchet for technical assistance.

Correspondence should be addressed to Laurent Groc, Unité Mixte de Recherche 5091, Centre National de la Recherche Scientifique, Université Bordeaux 2, 146 rue Léo Saignat, 33077 Bordeaux, France. E-mail: laurent.groc@u-bordeaux2.fr.

DOI:10.1523/JNEUROSCI.3349-07.2007

 0270-6474/07/2712433-05$15.00/0

approaches provided equivalent characteristics of receptor surface diffusion [e.g., for AMPA receptor in hippocampal cultured neurons (Adesnik et al., 2005; Ashby et al., 2006)], indicating that ensemble surface receptor diffusion can efficiently be measured using either approaches.

Opposite to the ensemble methods, single-molecule detection methods retrieve the diffusion properties of individual labeled receptors over time (Fig. 1*A*). The typical outcome is the complete distribution of the behavior of surface neurotransmitter receptors, which have revealed non-Gaussian shapes and a variety of diffusion characteristics at a given time. To date, this approach has unraveled the surface trafficking of neurotransmitter receptors and channels, including glutamatergic metabotropic mGluR5, AMPA and NMDA receptors (Borgdorff and Choquet, 2002; Serge et al., 2002; Tardin et al., 2003; Groc et al., 2004; Howarth et al., 2005; Groc et al., 2006), glycine (Meier et al., 2001; Dahan et al., 2003), GABA receptors (Bouzigues and Dahan, 2007), and Kv potassium channels (O'Connell et al., 2006). To label single molecules, there are essentially two possibilities: the use of a single dye (SD) or a single particle (SP) (e.g., nano-sized QDots). The SD tags are short lived but small size, whereas SP tags allow long observation times, but the size of the label can prevent its access to specific confined cellular areas.

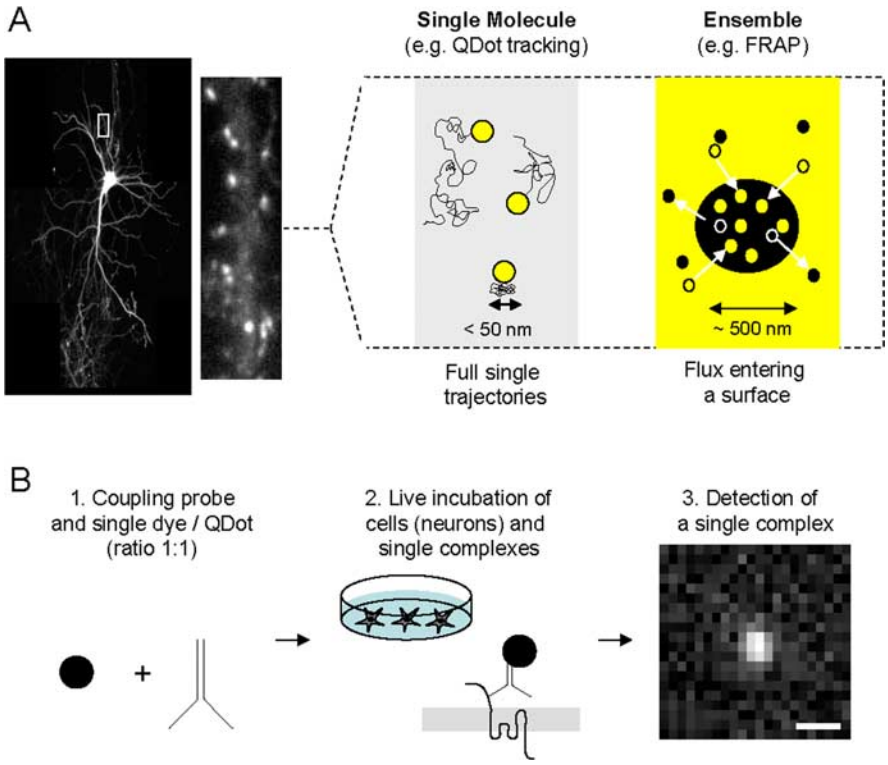

Figure 1. Schematic description of single-molecule/particle experiment for the tracking of surface receptors in neurons. ***A***, The first choice to make when planning to study receptors at the surface of neurons (left, hippocampal neuron expressing GFP-Homer 1C) is the type of experimental approach to setup. Right, There are schematically two ways to examine surface trafficking of receptors: ensemble or single-molecule approaches. The first one measures the surface behavior of the ensemble of labeled receptors using, for instance, FRAP. The second one measures the surface behavior of one (or possibly two if using antibody) receptor using single-molecule or Dot tracking. Although both approaches provide good measurements of receptor surface diffusion, differences in time and spatial resolutions exist. For instance, the spatial resolution in the type of microscopy used for FRAP and Dot experiments is defined by the diffraction limit, typically on the order of 200–300 nm. The single-molecule technique provides, however, a 10 nm pointing accuracy, which provides a unique way to collect the number of points necessary to build a trajectory in submicrometer membrane domains (e.g., synapse, lipid raft). ***B***, Experimental procedure to run single-molecule or Dot tracking. First, the label used to detect the molecule of interest (e.g., antibody) is coupled to the tag (single dye, single Dot) in the ratio 1:1 (left). Second, live neurons are incubated with the single tag complexes (high dilution, ~1 ng/ml) for several minutes. Third, single tag complexes are detected and tracked (see Single dye tracking and QDot tracking) over time as exemplified by the detection of a single Dot on a 30 ms acquisition image using a CCD camera. Scale bar, 600 nm. To ensure that the tracked complexes are in majority at the surface, rates of endocytosis of the receptor of interest should be first measured. SDT can then be performed during a time window in which only a low percentage (classically set as <15–20%) of receptors are internalized. For example, AMPAR surface tracking is performed only during 20 min after labeling, ensuring that <10–20% of labeled receptors are internalized. Note that the newly internalized AMPARs are mostly immobile and represent a small fraction of the single-molecule signals (Tardin et al., 2003).

Single dye tracking

SD tracking (SDT) first requires the attachment of a single tag (e.g., organic dye) to the molecular target through a specific high-affinity ligand that recognizes the extracellular domain of the molecular target in live cells (Fig. 1*B*). Labeling must be performed at low tag densities to be optically resolved (typically <1 molecule/μm^3) and to avoid cross-linking in the case of multivalent ligands (e.g., antibody). The second obvious requirement is to obtain signals from an SD that are large enough to overcome both the background noise from the molecule environment and that of the detection system (Fig. 1*B*). Several dyes fulfill these requirements, such as cyanine dyes (Cy3 or Cy5) that can be detected with good signal-to-noise ratios in live cells. The main limitation of SDT is, however, photobleaching, i.e., the processes by which photochemical reactions transform the excited fluorophore into a nonfluorescent product. It limits imaging time of a SD to typically a few seconds. Note that the use of antioxidant, such as Trolox, provides an efficient way to significantly reduce photobleaching and thus improve photostability (Rasnik et al., 2006).

In practice, single molecules are identified by their diffraction-limited signals, their well defined intensities, and the one-step photobleaching behavior (supplemental Box 1, available at www.jneurosci.org as supplemental material). Two-dimensional fitting by a Gaussian approximating the true point spread function of the microscope allows sub-wavelength localization of the labels (Cheezum et al., 2001), typically <50 nm for SDs in live cells (Tardin et al., 2003). Finally, once SDs are identified in each image frame, their two-dimensional trajectories can be constructed using a Vogel algorithm. This algorithm performs a correlation analysis between the positions of the SD found in consecutive images (Schmidt et al., 1995) (supplemental Box 2, available at www.jneurosci.org as supplemental material).

QDot tracking

QDots are passivated semiconductor nanocrystals that are water soluble and functionalized for biological applications. In addition to their superior brightness compared with SD, QDots have a larger absorption cross section, such that they can be excited with a mercury lamp. This allows recording large fields of view and

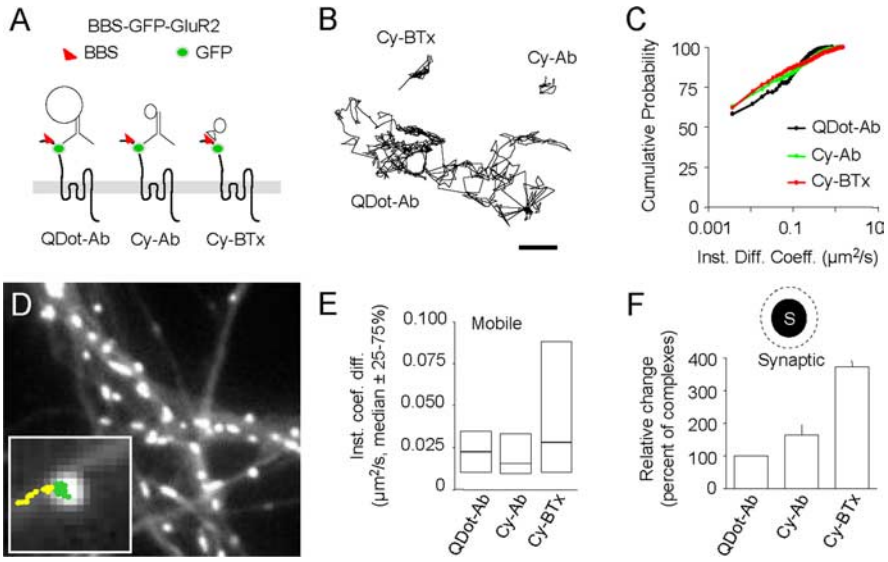

Figure 2. Tracking of a BBS-GFP-tagged GluR2 subunit using three different single-molecule/particle approaches. ***A***, Schematic representation of the BGG and the single-molecule/particle complexes: Dot coupled to antibody directed against GFP (left), cyanine 5 coupled to an antibody directed against GFP (center), and cyanine 5 coupled to bungarotoxin (right). The insertion of the BGG into the surface membrane was observed by incubating neurons transfected with BGG with bungarotoxin coupled to Alexa 568 (data not shown). Hippocampal neurons from 18-d-old rat embryos were cultured on glass coverslips following the Banker technique. For BGG expression, hippocampal neurons cultured 8–11 d *in vitro* were transfected with 1 μg of BGG cDNA for 24–36 h before the experiment using Lipofectamine 2000 reagent. Surface BGGs were detected by immunocytochemistry after live incubation with Alexa568-bungarotoxin (data not shown). Because cultured neurons can express low levels of endogenous nicotinic acetylcholine receptors, neurons were incubated with the nicotinergic receptor antagonist methyllycaconitine (10 nM, 20 min, 37°C) during single tag tracking. Finally, for single-molecule tracking, cyanine 3 or cyanine 5 was coupled to bungarotoxin or to the rabbit polyclonal anti-GFP antibody. For quantum dot (QD) tracking, QD 655 goat F(Ab')2 anti-rabbit IgGs (0.1 μM) were coupled with the polyclonal antibodies against GFP (1 μg). ***B***, Representative extrasynaptic trajectories from the three different surface single-molecule/particle complexes. Scale bar, 600 nm. Note the difference in trajectory length as a result of the photostability of single Dot when compared with cyanine 5 fluorophores. ***C***, Cumulative distributions of the instantaneous diffusion coefficient (bin size = 0.075 $\mu m^2/s$) ($p > 0.05$ for all comparisons, Kolmogorov–Smirnov test). The median values were not significantly different (QDot-Ab = 1×10^{-3} $\mu m^2/s$, IQR = 0–0.049 $\mu m^2/s$, $n = 1498$ trajectories; Cy-Ab = 2×10^{-3} $\mu m^2/s$, IQR = 1×10^{-4}–0.049 $\mu m^2/s$, $n = 919$; Cy-BTx = 4×10^{-3} $\mu m^2/s$, IQR = 0–0.025 $\mu m^2/s$, $n = 1387$; $p > 0.05$, Mann–Whitney *U* test). The percentage of immobile receptor (first point of the cumulative distribution) and the instantaneous diffusion coefficient (Inst. Diff. Coeff.) of the mobile molecules/particles (set to $D > 0.0075$ $\mu m^2/s$) were also not significantly different between complexes. All trajectories (each condition) were obtained from 30–60 dendritic fields and three to five different culture preparations. ***D***, Labeling of synapses using Mitotracker (1 min at 1 nM). Synaptic trajectories (green) are defined by their colocalization with synaptic labeling, the trajectory outside synapse being considered as extrasynaptic (yellow). Note the change in surface diffusion from a free diffusion behavior (extrasynaptic, yellow) to a confined one (synaptic, green). ***E***, Comparison of the instantaneous diffusion coefficient of mobile molecules/particles ($p < 0.05$, Mann-Whitney *U* test between Cy-BTx and the two other complexes). Note the subset of highly diffusing receptor detected with Cy-BTx. However, the instantaneous diffusion coefficient of all trajectories (QDot-Ab = 5×10^{-3} $\mu m^2/s$, IQR = 4×10^{-4}–0.023 $\mu m^2/s$, $n = 45$; Cy-Ab = 5×10^{-3} $\mu m^2/s$, IQR = 0–0.024 $\mu m^2/s$, $n = 98$; Cy-BTx = 10×10^{-3} $\mu m^2/s$, IQR = 7×10^{-4}–0.035 $\mu m^2/s$, $n = 51$; $p > 0.05$, Kruskal–Wallis test) and the percentage of immobile receptors ($p > 0.05$) were not significantly different between complexes. ***F***, Percentage of dyes/QDots detected within the synapse (QDot-Ab = 5.4 ± 1.3%, $n = 9$ dendritic areas; Cy-Ab = 9.4 ± 2.3%, $n = 33$; Cy-BTx = 20.3 ± 5.2%, $n = 35$; $p < 0.01$, ANOVA followed by Tukey's *post hoc* test). Note the relative increase toward smaller complexes.

gaining parallelism in data acquisition. Importantly, QDots are much more photostable than SDs, although they are subject to blinking (Michalet et al., 2005). However, these nanoparticles are still bigger than organic dyes and rather bulky (~10–30 nm).

Because of the larger signals obtained from QDots than from SDs, a faster detection algorithm than the two-dimensional Gaussian fitting of the luminescent signal was developed. It relies on wavelet transforms that filter the image frames and identify the QDots through their morphology and not their intensity. This algorithm provides minimal time and memory consumption and provides clear advantages when recording large images and very long QDot-based trajectories (supplemental Box 2, available at www.jneurosci.org as supplemental material). To account for the blinking of luminescent QDots, an algorithm was further used to reconnect iteratively portions of trajectories originating from the same QDots. The parameters of reconnection (maximum distance between reconnected events and maximum "dark" time) are adjusted according to the diffusion time of the molecules and the image acquisition rate. To prevent false reconnections, the surface density of QDots must be low enough that parameters of reconnection can be found without mixing the trajectories of different QDots. In practice, the maximum distance of reconnection is on the order of the mean QDot image-to-image steps and at least 10 times smaller than the mean distance between different QDots. It should be mentioned that other analytical approaches have been developed to overcome the problem of QDot blinking in trajectory reconstructions (Bonneau et al., 2005; Bachir et al., 2006). Interestingly, QDot blinking provides a criterion to identify individual QDots, because fluorescence changes between "on" and "off" states for a single Dot alternate only in two levels.

Does the size and valence of single tag complexes influence surface diffusion?

At the scale of the nano-sized probes, movements of surface extrasynaptic receptors are not governed by the mass of the probe, but instead by the motion of the membrane protein. Indeed, the viscosity of membranes is 100- to 1000-fold greater than that of extracellular medium. In restricted environments, however, like in the synaptic cleft, the size and valence of a single complex can impact surface receptor diffusion. The impact of different labeling strategies on SD/QDot measurements in nonconfined cellular environments (the extrasynaptic membrane) and confined ones (synapses labeled with Mitotracker) (Tardin et al., 2003; Groc et al., 2004) was measured. Cultured hippocampal neurons were transfected with the GluR2 AMPA receptor subunit tagged with a bungarotoxin binding site (BBS; 13 aa) and a GFP on an extracellular loop (Sekine-Aizawa and Huganir, 2004). The BBS-GFP-tagged GluR2 (BGG) subunits were then tracked at the neuronal surface using three different single-molecule complexes that have different sizes (QDot-Ab > Cy5-Ab > Cy5-BTx) and valences (QDot-Ab/Cy5-Ab/Cy5-BTx: 2/2/1), where QDot-Ab stands for QDots coupled to anti-GFP antibody (Ab, ~150 kDa); Cy5-Ab for a cyanine 5 (Cy5) coupled to anti-GFP antibody; and Cy5-BTx for a Cy5 coupled to bungarotoxin (BTx, 8 kDa) (Fig. 2*A*). The comparison of the diffusion of the three complexes in the extrasynaptic membrane revealed that the cumulative distributions of instantaneous

diffusion coefficients (Fig. 2*B*,*C*) and the median values of the total and mobile receptors were not significantly different.

Within synapses (Fig. 2*D*), the median values of instantaneous diffusion coefficients for all trajectories were also not significantly different, and neither were the percentage of immobile receptors (Fig. 2*E*). Interestingly, the distributions of the instantaneous diffusion coefficient for the only mobile receptors were different: Cy5-BTx complexes displayed a broader range than QDot-Ab and Cy5-Ab (Fig. 2*E*). Consistently, the median value of the Cy5-BTx distribution was significantly higher than the one of QDot-Ab and Cy5-Ab. Together, these results indicate that the three antibody-based complexes provide an equivalent picture of the proportion of diffusing synaptic receptors, although the smaller complex allow the additional visualization of a subset of highly diffusing receptors.

Regarding receptor diffusion within synaptic areas, two points should be discussed. First, synapses could be labeled using various markers, either presynaptic (e.g., Mitotracker, synaptotagmin) or postsynaptic (e.g., PSD-95, Homer 1c) (Tardin et al., 2003; Groc et al., 2004; Bats et al., 2007; Ehlers et al., 2007) (Figs. 1, 2). Comparing diffusion of AMPA receptors within synapses labeled with either Mitotracker (presynaptic) or Homer 1c (postsynaptic) shows almost similar diffusion characteristics (indistinguishable percentage of immobile receptors and exchange rate between extrasynaptic and synaptic membrane but a slight difference in the diffusion constant) (our unpublished data). Second, Dot functionalizing strategies can influence synaptic diffusion likely through difference in size and steric properties. For instance, diffusion distributions of synaptic GluR2 subunit are slower when measured with QDots coated with protein A (~50 kDa) [median = 0.005 $\mu m^2/s$, interquartile range (IQR; 25–75%) = 0.0005–0.03, $n = 59$] (Groc et al., 2004) compared with QDots coated with Fab fragment (20 kDa) (QDot-Fab: median = 0.025 $\mu m^2/s$, IQR = 0.0012–0.11, $n = 366$). In conclusion, all examined probes allow the tracking of synaptic receptors, but it appears that the smaller the probe, the better the tracking of fast diffusing synaptic receptors. This further encourages the development of very small probes (only few nanometers) for confined environments.

Do the different single-tagged complexes penetrate equally the synaptic cleft?

To answer this question, surface tag complexes were counted for each image series and were affected as extrasynaptic, synaptic, or juxtasynaptic (300–500 nm around the labeled synapses). In total, 150,584 molecules/particles were analyzed. The percentage of tag complexes localized within synapses (synaptic over total molecule number) averaged ~20% (range 0–26%). Interestingly, the synaptic content of Cy5-Ab and Cy5-BTx molecules was higher than that of QDot-Ab (Fig. 2*F*). However, in the juxtasynaptic membrane, this difference vanished, indicating that the size of single complexes is likely to affect the accessibility of the complexes to the highly confined synaptic cleft.

Are surface diffusions of endogenous and transfected receptor similar?

Recombinant receptor subunits are, and will be, widely used to study receptor trafficking during various paradigms of neuronal function. The simple but important question of whether endogenous and transfected receptors behave similarly at the neuronal surface appeared. The surface diffusion of both endogenous and transfected recombinant glutamatergic subunits were then compared using data collected from published (Groc et al., 2006; Bats et al., 2007) and unpublished (supplemental Box 3, available at www.jneurosci.org as supplemental material) studies. It emerged that overexpressed GluR or NR glutamatergic subunits exhibit either similar or different surface trafficking, respectively, when compared with endogenous ones. These results are only indicative for specific experimental designs and may vary with different transfection method, subunit types, or neuronal stages. Such comparison strongly suggests that pertinent controls (e.g., comparison between endogenous and recombinant subunit surface trafficking) should automatically be performed.

Future directions

What are the "ideal" probes for future single-molecule/particle tracking? The obvious and straightforward answer is to develop probes that are as small as possible, photoresistant, and with very limited blinking. Although the QDots are photoresistant and exhibit blinking, their actual multilayer water-stabilizing structure and coupling with antibodies (or streptavidin) results in tens-of-nanometers-size Dot complexes that equal the size of the synaptic cleft (results above). The engineering of smaller QDots, directly coupled to the detection probes (e.g., antibody or synthetic peptide), will surely improve the Dot-based complexes (Pinaud et al., 2004; Michalet et al., 2005). The tracking of individual few-nanometer gold particles in live neurons using a photothermal technique offers a promising alternative because it has the unique potential to record long trajectories (no theoretical limit) from very small probes (5 nm wide) (Lasne et al., 2006). As for the ligands, the engineering of small probes ($\ll$antibody or streptavidin) with high affinity will offer alternative ways, although the effects of recombinant subunit overexpression on cellular trafficking have to be carefully assayed. Finally, one aim of the cellular neuroscience field is to track receptors directly from live brains. Current roadblocks of this approach are based on *in vivo* imaging (multiphoton microscopy) of XFP-tag receptors in neurons that have been previously infected by virus (e.g., Sindbis virus, lentivirus) containing the XFP-tag receptor constructs (Svoboda and Yasuda, 2006). Whether pHluorin-XFP for ensemble measurements or QDots, organic molecules, and nanogold particles for single particle approaches will be the appropriate probes for receptor surface tracking *in vivo* remains an open and exciting question.

References

Adesnik H, Nicoll RA, England PM (2005) Photoinactivation of native AMPA receptors reveals their real-time trafficking. Neuron 48:977–985.

Ashby MC, Ibaraki K, Henley JM (2004) It's green outside: tracking cell surface proteins with pH-sensitive GFP. Trends Neurosci 27:257–261.

Ashby MC, Maier SR, Nishimune A, Henley JM (2006) Lateral diffusion drives constitutive exchange of AMPA receptors at dendritic spines and is regulated by spine morphology. J Neurosci 26:7046–7055.

Bachir A, Durisic N, Grutter P, Wiseman P (2006) Characterization of blinking dynamics in quantum dot ensembles using image correlation spectroscopy. J Appl Phys 99:064503.

Bats C, Groc L, Choquet D (2007) The interaction between Stargazin and PSD-95 regulates AMPA receptor surface trafficking. Neuron 53:719–734.

Bonneau S, Dahan M, Cohen L (2005) Single quantum dot tracking based on perceptual grouping using minimal paths in a spatiotemporal volume. IEEE Trans Image Process 14:1384–1395.

Borgdorff AJ, Choquet D (2002) Regulation of AMPA receptor lateral movements. Nature 417:649–653.

Bouzigues C, Dahan M (2007) Transient di-

rected motions of GABA(A) receptors in growth cones detected by a speed correlation index. Biophys J 92:654–660.

Bredt DS, Nicoll RA (2003) AMPA receptor trafficking at excitatory synapses. Neuron 40:361–379.

Cheezum M, Walker W, Guilford W (2001) Quantitative comparison of algorithms for tracking single fluorescent particles. Biophys J 81:2378–2388.

Cognet L, Coussen F, Choquet D, Lounis B (2002) Fluorescence microscopy of single autofluorescent proteins for cellular biology. C R Acad Sci IV 3:645–656.

Dahan M, Levi S, Luccardini C, Rostaing P, Riveau B, Triller A (2003) Diffusion dynamics of glycine receptors revealed by single-quantum dot tracking. Science 302:442–445.

Ehlers MD, Heine M, Groc L, Lee MC, Choquet D (2007) Diffusional trapping of GluR1 AMPA receptors by input-specific synaptic activity. Neuron 54:447–460.

Groc L, Choquet D (2006) AMPA and NMDA glutamate receptor trafficking: multiple roads for reaching and leaving the synapse. Cell Tissue Res 326:423–438.

Groc L, Heine M, Cognet L, Brickley K, Stephenson FA, Lounis B, Choquet D (2004) Differential activity-dependent regulation of the lateral mobilities of AMPA and NMDA receptors. Nat Neurosci 7:695–696.

Groc L, Heine M, Cousins SL, Stephenson FA, Lounis B, Cognet L, Choquet D (2006) NMDA receptor surface mobility depends on NR2A–2B subunits. Proc Natl Acad Sci USA 103:18769–18774.

Howarth M, Takao K, Hayashi Y, Ting AY (2005) Targeting quantum dots to surface proteins in living cells with biotin ligase. Proc Natl Acad Sci USA 102:7583–7588.

Kennedy MJ, Ehlers MD (2006) Organelles and trafficking machinery for postsynaptic plasticity. Annu Rev Neurosci 29:325–362.

Kopec CD, Li B, Wei W, Boehm J, Malinow R (2006) Glutamate receptor exocytosis and spine enlargement during chemically induced long-term potentiation. J Neurosci 26:2000–2009.

Lasne D, Blab GA, Berciaud S, Heine M, Groc L, Choquet D, Cognet L, Lounis B (2006) Single nanoparticle photothermal tracking (SNaPT) of 5-nm gold beads in live cells. Biophys J 91:4598–4604.

Lippincott-Schwartz J, Patterson GH (2003) Development and use of fluorescent protein markers in living cells. Science 300:87–91.

Lober RM, Pereira MA, Lambert NA (2006) Rapid activation of inwardly rectifying potassium channels by immobile G-protein-coupled receptors. J Neurosci 26:12602–12608.

Meier J, Vannier C, Serge A, Triller A, Choquet D (2001) Fast and reversible trapping of surface glycine receptors by gephyrin. Nat Neurosci 4:253–260.

Michalet X, Pinaud FF, Bentolila LA, Tsay JM, Doose S, Li JJ, Sundaresan G, Wu AM, Gambhir SS, Weiss S (2005) Quantum dots for live cells, in vivo imaging, and diagnostics. Science 307:538–544.

O'Connell KMS, Rolig AS, Whitesell JD, Tamkun MM (2006) Kv2.1 potassium channels are retained within dynamic cell surface microdomains that are defined by a perimeter fence. J Neurosci 26:9609–9618.

Pinaud F, King D, Moore HP, Weiss S (2004) Bioactivation and cell targeting of semiconductor CdSe/ZnS nanocrystals with phytochelatin-related peptides. J Am Chem Soc 126:6115–6123.

Rasnik I, McKinney SA, Ha T (2006) Nonblinking and long-lasting single-molecule fluorescence imaging. Nat Methods 3:891–893.

Rasse TM, Fouquet W, Schmid A, Kittle RJ, Mertel S, Sigrist CB, Schmidt M, Guzman A, Merino C, Qin G, Quentin C, Madeo FF, Heckmann M, Sigrist SJ (2005) Glutamate receptor dynamics organizing synapse formation in vivo. Nat Neurosci 8:898–905.

Schmidt T, Schutz GJ, Baumgartner W, Gruber HJ, Schindler H (1995) Characterization of photophysics and mobility of single molecules in a fluid lipid membrane. J Phys Chem 99:17662–17668.

Sekine-Aizawa Y, Huganir RL (2004) Imaging of receptor trafficking by using alpha-bungarotoxin-binding-site-tagged receptors. Proc Natl Acad Sci USA 101:17114–17119.

Serge A, Fourgeaud L, Hemar A, Choquet D (2002) Receptor activation and homer differentially control the lateral mobility of metabotropic glutamate receptor 5 in the neuronal membrane. J Neurosci 22:3910–3920.

Sharma K, Fong DK, Craig AM (2006) Postsynaptic protein mobility in dendritic spines: long-term regulation by synaptic NMDA receptor activation. Mol Cell Neurosci 31:702–712.

Svoboda K, Yasuda R (2006) Principles of two-photon excitation microscopy and its applications to neuroscience. Neuron 50:823–839.

Tardin C, Cognet L, Bats C, Lounis B, Choquet D (2003) Direct imaging of lateral movements of AMPA receptors inside synapses. EMBO J 22:4656–4665.

Thomas P, Mortensen M, Hosie AM, Smart TG (2005) Dynamic mobility of functional GABAA receptors at inhibitory synapses. Nat Neurosci 8:889–897.

Tovar KR, Westbrook GL (2002) Mobile NMDA receptors at hippocampal synapses. Neuron 34:255–264.